Radiation Physics and Chemistry 194 (2022) 110039

Contents lists available at ScienceDirect

Radiation Physics and Chemistry

journal homepage: www.elsevier.com/locate/radphyschem

Micro Pb filled polymer composites: Theoretical, experimental and simulation results for γ-ray shielding performance

O. Kilicoglu [a], Chaitali V. More [b], F. Akman [c,d,*], K. Dilsiz [e], H. Oğul [f], M.R. Kaçal [g], H. Polat [h], O. Agar [i]

[a] Radiation Laboratory, University of Notre Dame, Notre Dame, IN, 46556-5670, USA
[b] Department of Physics, Dr. Babasaheb Ambedkar Marathwada University, Aurangabad, India
[c] Bingöl University, Vocational School of Social Sciences, Department of Property Protection and Security, Program of Occupational Health and Safety, 12000, Bingöl, Turkey
[d] Bingöl University, Central Laboratory Application and Research Center, 12000, Bingöl, Turkey
[e] Bingöl University, Faculty of Art and Science, Department of Physics, 12000, Bingöl, Turkey
[f] Department of Nuclear Engineering, Faculty of Engineering and Architecture, Sinop University, Sinop, Turkey
[g] Giresun University, Arts and Sciences Faculty, Department of Physics, 28100, Giresun, Turkey
[h] Bingöl University, Vocational School of Technical Sciences, Department of Architecture and Urban Planning, 12000, Bingöl, Turkey
[i] Karamanoğlu Mehmetbey University, Department of Medical Imaging Techniques, 70100, Karaman, Turkey

ARTICLE INFO

Keywords:
FLUKA
GEANT4
HPGe detector
Buildup factor
Gamma shielding

ABSTRACT

Researches on advanced composites to protect environment health towards radioactive pollution have drawn attention with the rising use of radioactive elements. From this point, polymer micro composites are quite encouraging in terms of multifunctional properties in mechanical, electrical, thermal, as well as nuclear shielding. The present study has explored the efficacy of micro lead (Pb) loaded polymer composites for radio protective applications such as a fabrication of protective enclosures. High energetic photon shielding experiments have been applied through gamma spectrometer equipped with HPGe detector and various radioactive point sources namely ^{137}Cs, ^{22}Na, ^{152}Eu, ^{133}Ba, ^{241}Am and ^{57,60}Co which are widely used in several medical and industrial applications. The results demonstrated that mass attenuation coefficients of the composites at different photon energies are proportional to the filler loading. The validation of FLUKA and GEANT4 Monte Carlo software has been performed in the simulation of transmission experiments as well as WinXCOM software. The tests of the Pb (20%) micro composite for the nuclear radiation shielding reveal that it has high attenuation coefficients for photon radiation.

1. Introduction

Availability of effective radiation shielding materials enables the safe usage of the applications containing ionizing radiation especially gamma-rays and radioactive sources. In this context, advancements in efficacious radiation shielding materials have gained a significant importance, which motivates the researchers working in the field of nuclear radiation to continuously search and fabricate new radiation shields that are alternative to conventional radiation shields (Aldhuhaibat et al., 2021; More et al., 2021). Some of these studies are focused on developing composite materials by incorporation of various filler materials in various matrices so that the various properties of these materials will be merged and one effective composite radiation shield will be formed. In this regard, polymers could be given as an example: highly valued matrix materials in order to advance light weight, durable and flexible γ-ray shields. In addition, polymer composites have merits over metals such as its superiority in workability, flexibility, low cost, chemical stability, volume diminishment after use etc. (Aldhuhaibat et al., 2021; Alavian and Tavakoli-Anbaran, 2020; Afshar et al., 2019; Bedar et al., 2019). Furthermore, polymeric materials may be convenient for neutron scatters in which contains high numbers of H, and amalgamating this property with use of some additives such as high atomic number materials, polymers could become an appropriate candidate for shielding of γ- and X-rays (Kaçal et al., 2019; Azman et al.,

* Corresponding author. Bingöl University, Vocational School of Social Sciences, Department of Property Protection and Security, Program of Occupational Health and Safety, 12000, Bingöl, Turkey.
E-mail address: fakman@bingol.edu.tr (F. Akman).

https://doi.org/10.1016/j.radphyschem.2022.110039
Received 20 June 2021; Received in revised form 28 November 2021; Accepted 16 February 2022
Available online 21 February 2022

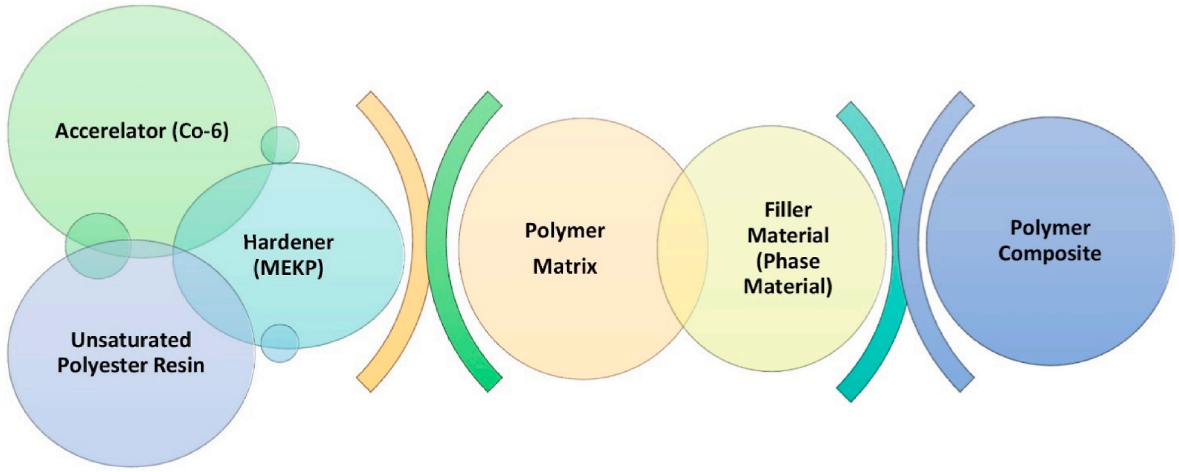

Fig. 1. Schematic representation of the sample production process.

Table 1
The elemental compositions and densities of the Pb doped polymer composites.

Sample	Compositions (%)					ρ (g/cm^3)
	H	C	O	Co	Pb	
Pb (5%)	4.4475	56.9947	34.0057	0.0271	4.5249	1.3903
Pb (10%)	4.2550	54.5274	32.5336	0.0260	8.6580	1.4015
Pb (15%)	4.0785	52.2649	31.1837	0.0249	12.4481	1.4233
Pb (20%)	3.9160	50.1826	29.9413	0.0239	15.9363	1.4652

2013). All of these outstanding properties have made polymer composites crucial in execution of radiation-shielding.

The polymer matrix for the present investigation was chosen as unsaturated polyester resin (UPR), and lead (Pb) was used as a filler material. Here, it should be noted that UPR is gaining utmost attention by virtue of wide range of applications in land transportation industries, marine, construction, aerospace, electronic devices, waterlines and automotive due to its superior properties such as good thermal stability, low cost, ease of fabrication, and high-performance properties which makes it versatile and significant material (Abu-Jdayil et al., 2019; Ambika et al., 2017). Additionally, UPR is an extraordinary multipurpose thermoset material used as polymer matrix in composites. On the other hand, there are various studies on the radiation attenuation features of Pb-doped some materials to minimize the damage of lead and to increase the shielding properties of the studied materials (Tekin et al., 2019; Singh et al., 2004; Kumar et al., 2020; Mansy et al., 2021; Hassan et al., 2015). A brief motivation for choosing Pb as a filler could be introduced with following studies. An earlier investigation on composites reported that lead monoxide (PbO) is a good filler with its incorporation in concrete and polymer matrices (Özdemir et al., 2018). In other words, γ-ray attenuation properties of concrete were improved by the addition of PbO nanoparticles into the concrete (Özdemir et al., 2018). In another study, the ethylene propylene diene terpolymer (EPDM) was examined and used as polymeric matrix along with PbO nano particles and bismuth oxide particles for different weight ratios as radiation shielding functional materials (Harish et al., 2012). γ-ray shielding capabilities of isophthalic resin (ISO) composites incorporated with three types of lead oxides (PbO, PbO_2, and Pb_3O_4) at various weight fractions were evaluated, and it was concluded that the ISO composites filled with PbO were more effective for radiation shielding than their counterparts (Harish et al., 2012). Similarly, Belgin et al. (2015) reported a study in which different ratios of powdered PbO and WO_3 were incorporated in linear low density-polyethylene to form an effective composite material and attenuate ionizing electromagnetic radiation. On another study, unsaturated polyester composites containing 5 wt% nano clay and different wt% of PbO particles were tested and the results showed that they were better than the other composites in γ-ray shielding at low energies (Bagheri et al., 2018). Other studies investigated the composites of PbO infused unsaturated polyester for their

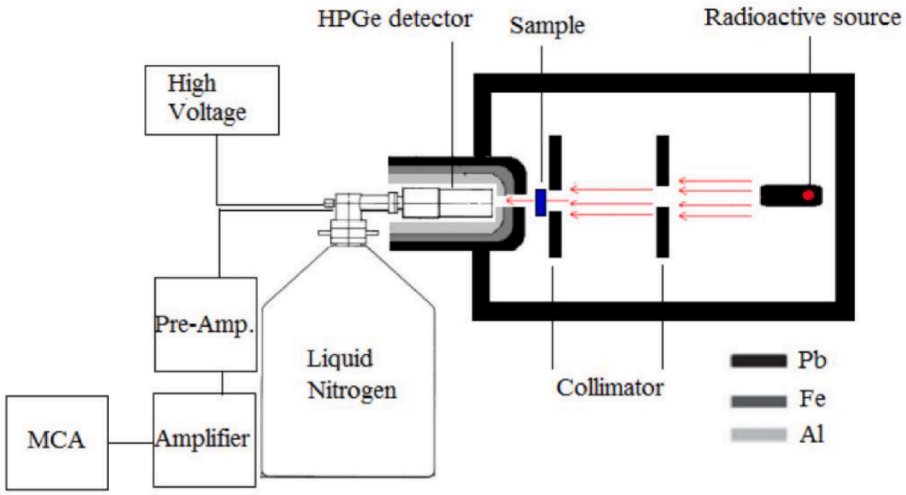

Fig. 2. Schematic diagram of experimental setup.

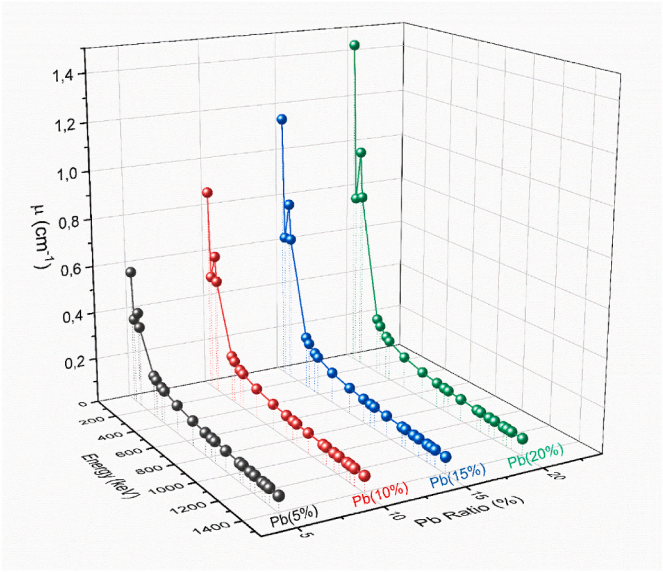

Fig. 3. The theoretical values of the linear attenuation coefficient as a function of photon energy.

γ-ray protection efficiency and found these materials to be a good alternate candidate for radiological protection (Harish et al., 2009, 2010).

In short, the present study aims to develop cost-effective, durable, low-weight polymer composite radiation shields by incorporation of different amounts (5, 10, 15 and 20 wt%) of Pb micro particles. The experiments have been executed using HPGe detector and different radioactive sources in the energy range of 59.5–1408.0 keV. Mass attenuation coefficient (μ/ρ) of the investigated samples were obtained using this experimental geometry. This measured attenuation coefficient data is further used to determine other radiological parameters including linear attenuation coefficient (μ), effective atomic and electron number (Z_{eff} and N_E), mean free path (MFP), half value layer (HVL), tenth value layer (TVL) and radiation protection efficiency (RPE). The experimental results of these parameters have been validated by the theoretical values based on WinXCom, FLUKA and GEANT4 Monte Carlo simulation codes. KERMA factor has also evaluated and its variation with energy has been reported. Energy absorption and exposure buildup factors (EABF and EBF) of the chosen samples have been computed using geometric progression (G-P) fitting method.

The methodology of this article is as follows: The theoretical context of photon-matter interactions is provided in Section 2. Section 3 reviews the experimental details and its validation with WinXCom, FLUKA and GEANT4 simulation data. The comparisons between the experimental, theoretical and simulated results are outlined in Section 4. Section 5 concludes the performed investigation.

2. Theoretical context

The theoretical framework used to calculate γ-rays shielding parameters have been outlined as follows.

2.1. Linear attenuation and mass attenuation coefficients

The linear attenuation coefficient is the probability of interaction between radiation and matter per path length while the mass attenuation coefficient is the fundamental parameter used to determine other radiological parameters such as effective atomic number and electron density, half value layer, tenth value layer and mean free path.

$$\frac{\mu}{\rho} = \left(-\frac{1}{\rho x}\right) \ln \frac{I}{I_0} \tag{1}$$

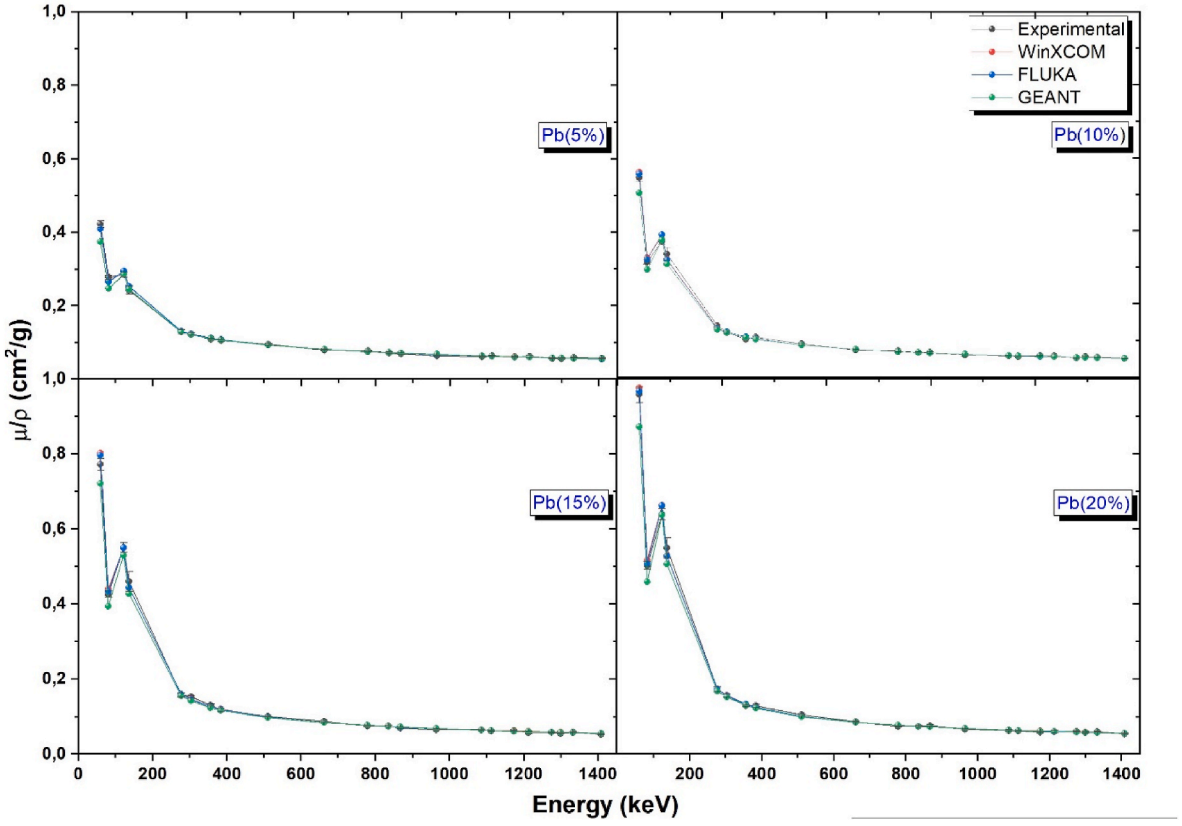

Fig. 4. Experimental, WinXCOM, FLUKA and GEANT4 mass attenuation coefficients obtained for the fabricated micro-composites.

Table 2
μ/ρ ($cm^2\ g^{-1}$) results for experimental, WinXCOM, FLUKA and GEANT4 of Pb doped polymer composites.

Energy (keV)	Pb (5%)				Pb (10%)				Pb (15%)				Pb (20%)			
	Exp.	WinX	FLUKA	GEANT4	Exp.	WinX.	FLUKA	GEANT4	Exp.	WinX.	FLUKA	GEANT4	Exp.	WinX.	FLUKA	GEANT4
59.5	0.4223 ± 0.0087	0.4096	0.4100	0.3750	0.6009 ± 0.0125	0.6168	0.6117	0.5553	0.7716 ± 0.0164	0.8018	0.7965	0.7210	0.9579 ± 0.0210	0.9757	0.9673	0.8728
81.0	0.2779 ± 0.0057	0.2673	0.2660	0.2476	0.3468 ± 0.0071	0.3587	0.3539	0.3237	0.4256 ± 0.0088	0.4403	0.4341	0.3942	0.5021 ± 0.0104	0.5171	0.5082	0.4588
122.1	0.2855 ± 0.0066	0.2941	0.2954	0.2856	0.4087 ± 0.0095	0.4289	0.4282	0.4130	0.5503 ± 0.0130	0.5493	0.5503	0.5296	0.6384 ± 0.0153	0.6625	0.6619	0.6372
136.5	0.2435 ± 0.0114	0.2529	0.2536	0.2457	0.3707 ± 0.0192	0.3537	0.3525	0.3400	0.4598 ± 0.0264	0.4438	0.4438	0.4271	0.5490 ± 0.0260	0.5284	0.5272	0.5065
276.4	0.1302 ± 0.0046	0.1314	0.1315	0.1292	0.1541 ± 0.0050	0.1467	0.1462	0.1431	0.1576 ± 0.0057	0.1603	0.1598	0.1561	0.1732 ± 0.0061	0.1732	0.1733	0.1677
302.9	0.1239 ± 0.0030	0.1240	0.1239	0.1221	0.1349 ± 0.0033	0.1359	0.1356	0.1329	0.1531 ± 0.0037	0.1466	0.1463	0.1428	0.1565 ± 0.0040	0.1566	0.1562	0.1518
356.0	0.1090 ± 0.0023	0.1128	0.1128	0.1114	0.1132 ± 0.0024	0.1205	0.1201	0.1183	0.1305 ± 0.0027	0.1273	0.1271	0.1243	0.1292 ± 0.0027	0.1338	0.1333	0.1300
383.9	0.1057 ± 0.0034	0.1082	0.1081	0.1073	0.1194 ± 0.0039	0.1144	0.1142	0.1127	0.1178 ± 0.0037	0.1200	0.1199	0.1176	0.1287 ± 0.0042	0.1252	0.1250	0.1223
511.0	0.0959 ± 0.0020	0.0933	0.0932	0.0931	0.0990 ± 0.0020	0.0961	0.0960	0.0954	0.1011 ± 0.0021	0.0985	0.0982	0.0975	0.1053 ± 0.0022	0.1009	0.1006	0.0995
661.7	0.0803 ± 0.0017	0.0821	0.0821	0.0822	0.0810 ± 0.0017	0.0833	0.0833	0.0832	0.0874 ± 0.0018	0.0844	0.0843	0.0840	0.0864 ± 0.0018	0.0854	0.0852	0.0849
778.9	0.0777 ± 0.0020	0.0757	0.0755	0.0759	0.0778 ± 0.0020	0.0764	0.0764	0.0763	0.0751 ± 0.0020	0.0770	0.0769	0.0769	0.0737 ± 0.0019	0.0776	0.0773	0.0772
834.8	0.0725 ± 0.0018	0.0731	0.0731	0.0734	0.0736 ± 0.0018	0.0736	0.0736	0.0737	0.0753 ± 0.0019	0.0741	0.0740	0.0740	0.0746 ± 0.0018	0.0745	0.0742	0.0743
867.4	0.0704 ± 0.0027	0.0717	0.0717	0.0718	0.0729 ± 0.0027	0.0722	0.0721	0.0723	0.0702 ± 0.0024	0.0725	0.0725	0.0725	0.0765 ± 0.0028	0.0729	0.0727	0.0726
964.1	0.0648 ± 0.0014	0.0680	0.0680	0.0683	0.0652 ± 0.0014	0.0682	0.0681	0.0684	0.0658 ± 0.0015	0.0685	0.0684	0.0685	0.0659 ± 0.0015	0.0687	0.0686	0.0687
1085.9	0.0618 ± 0.0016	0.0640	0.0639	0.0641	0.0637 ± 0.0016	0.0641	0.0640	0.0640	0.0650 ± 0.0017	0.0642	0.0640	0.0641	0.0633 ± 0.0016	0.0643	0.0642	0.0640
1112.1	0.0642 ± 0.0014	0.0633	0.0632	0.0634	0.0612 ± 0.0013	0.0633	0.0631	0.0632	0.0624 ± 0.0013	0.0634	0.0633	0.0631	0.0615 ± 0.0013	0.0634	0.0634	0.0632
1173.2	0.0614 ± 0.0013	0.0615	0.0615	0.0615	0.0649 ± 0.0014	0.0615	0.0613	0.0616	0.0632 ± 0.0013	0.0615	0.0614	0.0614	0.0587 ± 0.0012	0.0615	0.0614	0.0613
1212.9	0.0628 ± 0.0030	0.0604	0.0604	0.0606	0.0633 ± 0.0033	0.0604	0.0605	0.0605	0.0576 ± 0.0028	0.0604	0.0603	0.0604	0.0601 ± 0.0028	0.0604	0.0603	0.0604
1274.5	0.0579 ± 0.0012	0.0589	0.0588	0.0591	0.0571 ± 0.0012	0.0588	0.0586	0.0589	0.0582 ± 0.0012	0.0588	0.0586	0.0588	0.0612 ± 0.0013	0.0588	0.0587	0.0589
1299.1	0.0569 ± 0.0021	0.0583	0.0583	0.0584	0.0615 ± 0.0023	0.0583	0.0582	0.0583	0.0560 ± 0.0021	0.0582	0.0582	0.0581	0.0584 ± 0.0023	0.0582	0.0580	0.0580
1332.5	0.0594 ± 0.0012	0.0575	0.0575	0.0576	0.0590 ± 0.0012	0.0575	0.0574	0.0575	0.0588 ± 0.0012	0.0574	0.0573	0.0574	0.0594 ± 0.0012	0.0574	0.0573	0.0574
1408.0	0.0577 ± 0.0012	0.0559	0.0558	0.0560	0.0552 ± 0.0011	0.0558	0.0557	0.0559	0.0534 ± 0.0011	0.0558	0.0556	0.0557	0.0539 ± 0.0011	0.0557	0.0556	0.0556

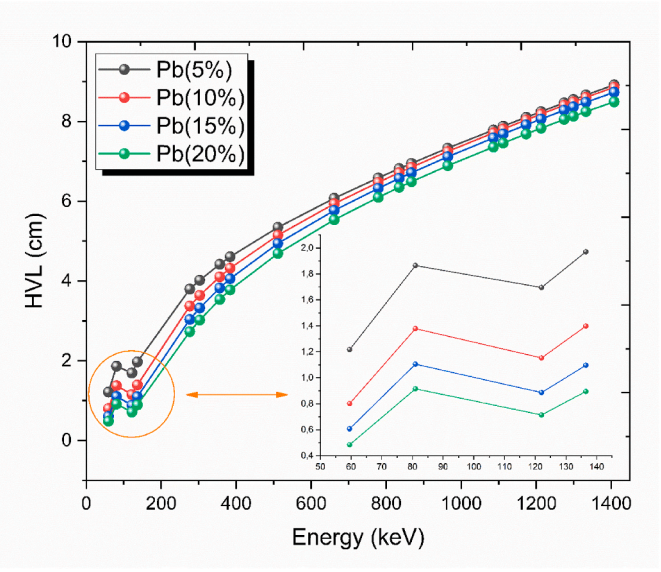

Fig. 5. Half value layer (HVL) values as a function of photon energy.

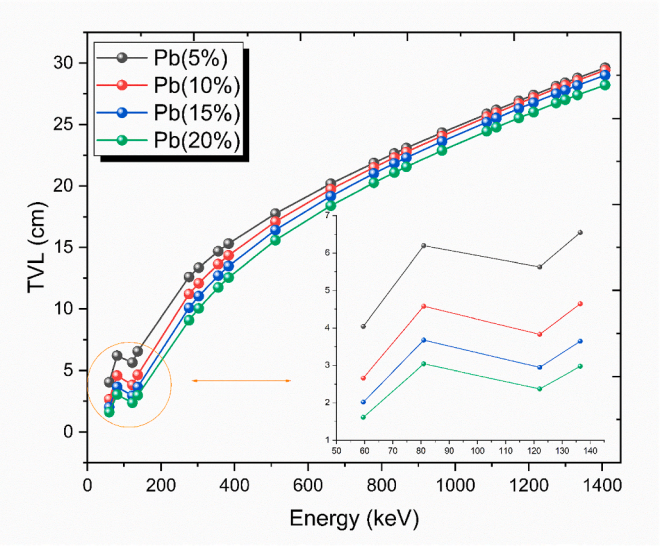

Fig. 6. Tenth value layer (TVL) values as a function photon energy.

where x, I_0 and I are the thickness of absorbing material, initial and transmitted intensity of radiation. The total mass attenuation coefficient (μ_{tot}) for a given photon energy could be defined as Equation (2),

$$\mu_{tot} = \mu_{pe} + \mu_{comp} + \mu_{pp} \tag{2}$$

where pe, comp and pp are photoelectric absorption, Compton scattering, and pair production (Sharma et al., 2020).

2.2. Half value layer and tenth value layer

HVL and TVL are handy parameters used for the quick determination of shielding efficiency of a material. The linear attenuation coefficient of a material is always related to HVL and TVL by the following equations (More et al., 2020a),

$$HVL = \frac{\ln 2}{\mu} \tag{3}$$

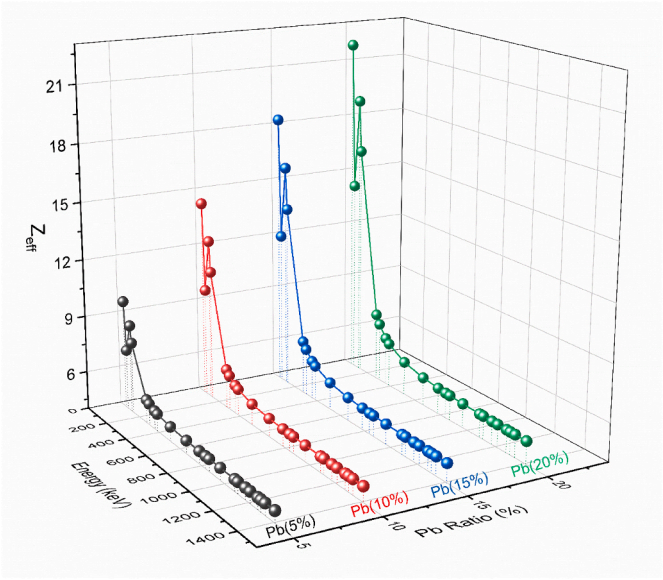

Fig. 7. Effective atomic number (Z_{eff}) values as a function of photon energy and Pb-content of the samples.

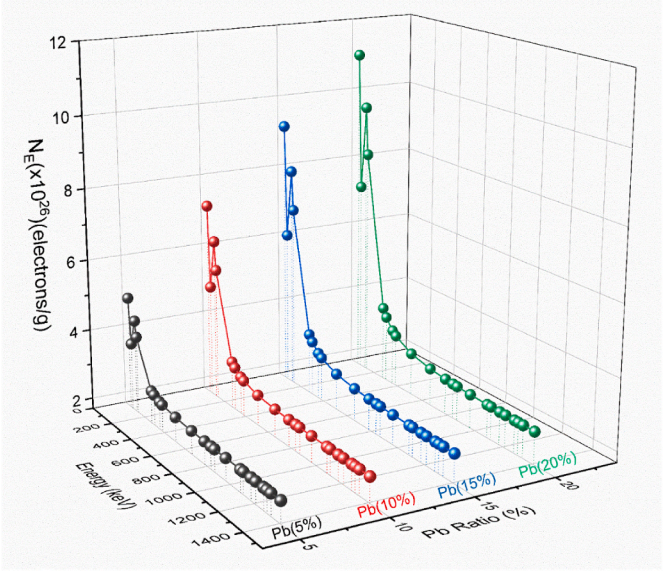

Fig. 8. Effective electron density (N_E) values as a function of photon energy and Pb-content of the samples.

$$TVL = \frac{\ln 10}{\mu} \tag{4}$$

2.3. Mean free path

Mean free path, which is also known as relaxation length (λ), is the mean excursion between two successive interactions of photons and it is denoted by the expression,

$$MFP = \frac{1}{\mu} \tag{5}$$

2.4. Effective atomic number and electron density

Effective atomic number of polymer composites is given by relation,

$$Z_{eff} = \frac{\sigma_a}{\sigma_{el}} \tag{6}$$

where σ_a and σ_{el} are total atomic cross-section and total electronic cross-section, respectively and these are computed by the following equations,

$$\sigma_a = \frac{1}{N_A}\sum_i f_i A_i(\mu_m) \tag{7}$$

$$\sigma_{el} = \frac{1}{N_A}\sum_i \frac{f_i A_i}{Z_i}(\mu_m)_i \tag{8}$$

The effective electron density (N_E) is related to the Z_{eff} as;

$$N_E = N_A \frac{Z_{eff}}{A_{eff}} \tag{9}$$

where $f_i = n_i / \sum n_i$ is the fractional abundance of ith element with respect to the number of atoms such that $\sum_i^n f_i = 1$; A_i, and Z_i are the atomic weight, and the atomic number of ith element in a matter (More et al., 2020b).

2.5. Radiation protection efficiency

The radiation protection efficiency is an important parameter which determines effectiveness of a shielding material and is given as follows:

$$\mathrm{RPE} = \left(1 - \frac{I}{I_0}\right) \times 100 \tag{10}$$

2.6. KERMA relative to air (K_a)

Kerma (kinetic energy released per unit mass) is non-stochastic quantity which is applicable to photons (X-, γ-rays, etc.) and neutrons. The expression for kerma is given as:

$$K = \psi(\mu_{en}/\rho) \tag{11}$$

where ψ and (μ_{en}/ρ) are the energy fluence of mono-energetic photons and mass energy coefficient, respectively. Kerma relative to air of a material is given by relation below (Manohara et al., 2008):

$$K_a = \frac{(\mu_{en}/\rho)_{mat}}{(\mu_{en}/\rho)_{air}} \tag{12}$$

The values of mass energy-absorption coefficients for air and elemental constituents of materials have been taken from the compilation of NIST data (Hubbell and Seltzer, 1995).

2.7. Energy absorption and exposure buildup factors

Buildup factor, a significant parameter in gamma ray shielding calculations, that determines corrected response to uncollided photons by including the contribution of any scattered and secondary photons (Singh et al., 2014; Vahabi and Zafarghandi, 2020). Exposure build-up factor (EBF) and energy absorption build-up factor (EABF) have been determined using well known G–P fitting method which has been discussed in detail in ref (More et al., 2021).

3. Experimental details and its validation

3.1. Production of composites

In this study, polipol 314 filling type polyester resin and methyl, ethyl, ketone and peroxide (MEKP) having 1.113 and 1.17 g/cm^3 were used respectively. Due to some advantages such as fast gelation, curing feature and at room temperature, it is quite convenient to obtain the curing resins in combination with MEKP and Cobalt Octoate (6%) accelerator with 0.885 g/cm^3. Initially, the polymer matrix has been

Table 3
Experimental and theoretical Z_{eff} results of Pb doped polymer composites.

Energy (keV)	Pb (5%)		Pb (10%)		Pb (15%)		Pb (20%)	
	Exp.	Theo.	Exp.	Theo.	Exp.	Theo.	Exp.	Theo.
59.5	10.0101 ± 0.2065	9.7108	13.9487 ± 0.2903	14.3198	17.5871 ± 0.3730	18.2769	21.4689 ± 0.4706	21.8685
81.0	7.4398 ± 0.1530	7.1549	9.3801 ± 0.1932	9.7019	11.6179 ± 0.2402	12.0213	13.8292 ± 0.2874	14.2420
122.1	8.3740 ± 0.1922	8.6262	11.8816 ± 0.2775	12.4702	15.8740 ± 0.3748	15.8456	18.2832 ± 0.4370	18.9715
136.5	7.4610 ± 0.3478	7.7499	11.3826 ± 0.5894	10.8629	14.1474 ± 0.8129	13.6537	16.9219 ± 0.8021	16.2874
276.4	5.1900 ± 0.1834	5.2379	6.3595 ± 0.2053	6.0520	6.7127 ± 0.2410	6.8285	7.6087 ± 0.2698	7.6056
302.9	5.1148 ± 0.1236	5.1192	5.7737 ± 0.1395	5.8170	6.7736 ± 0.1649	6.4846	7.1519 ± 0.1847	7.1547
356.0	4.7932 ± 0.0998	4.9617	5.1738 ± 0.1077	5.5043	6.1751 ± 0.1292	6.0254	6.3272 ± 0.1315	6.5507
383.9	4.7939 ± 0.1539	4.9058	5.6294 ± 0.1823	5.3929	5.7536 ± 0.1797	5.8615	6.5099 ± 0.2141	6.3344
511.0	4.8966 ± 0.1004	4.7624	5.2593 ± 0.1080	5.1063	5.5795 ± 0.1147	5.4384	6.0300 ± 0.1239	5.7747
661.7	4.5917 ± 0.0945	4.6905	4.8244 ± 0.0990	4.9628	5.4136 ± 0.1112	5.2262	5.5561 ± 0.1142	5.4935
778.9	4.7850 ± 0.1249	4.6616	4.9932 ± 0.1311	4.9048	5.0121 ± 0.1313	5.1402	5.1134 ± 0.1342	5.3794
834.8	4.6100 ± 0.1145	4.6519	4.8816 ± 0.1203	4.8854	5.1975 ± 0.1290	5.1114	5.3431 ± 0.1319	5.3410
867.4	4.5587 ± 0.1736	4.6471	4.9288 ± 0.1846	4.8757	4.9318 ± 0.1680	5.0970	5.5839 ± 0.2034	5.3219
964.1	4.4168 ± 0.0981	4.6355	4.6364 ± 0.1029	4.8523	4.8657 ± 0.1083	5.0624	5.0663 ± 0.1123	5.2759
1085.9	4.4627 ± 0.1168	4.6248	4.7964 ± 0.1224	4.8310	5.0921 ± 0.1322	5.0309	5.1572 ± 0.1318	5.2341
1112.1	4.6898 ± 0.1008	4.6231	4.6656 ± 0.1001	4.8275	4.9517 ± 0.1064	5.0256	5.0714 ± 0.1090	5.2271
1173.2	4.6074 ± 0.0972	4.6197	5.0821 ± 0.1071	4.8206	5.1525 ± 0.1087	5.0152	4.9734 ± 0.1049	5.2132
1212.9	4.7959 ± 0.2330	4.6180	5.0453 ± 0.2666	4.8169	4.7758 ± 0.2315	5.0097	5.1778 ± 0.2409	5.2058
1274.5	4.5421 ± 0.0946	4.6159	4.6698 ± 0.0971	4.8125	4.9508 ± 0.1031	5.0030	5.4137 ± 0.1129	5.1968
1299.1	4.5060 ± 0.1669	4.6153	5.0783 ± 0.1938	4.8111	4.8066 ± 0.1817	5.0010	5.2148 ± 0.2085	5.1941
1332.5	4.7649 ± 0.0994	4.6145	4.9409 ± 0.1027	4.8096	5.1152 ± 0.1064	4.9986	5.3723 ± 0.1118	5.1908
1408.0	4.7647 ± 0.0977	4.6136	4.7546 ± 0.0975	4.8073	4.7863 ± 0.0982	4.9951	5.0194 ± 0.1030	5.1860

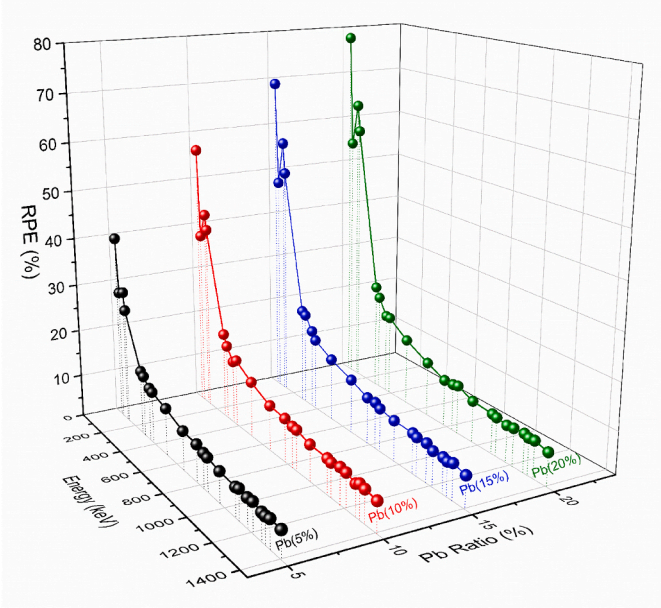

Fig. 9. Radiation protection efficiencies (RPEs) as a function of photon energy and Pb-content of the samples.

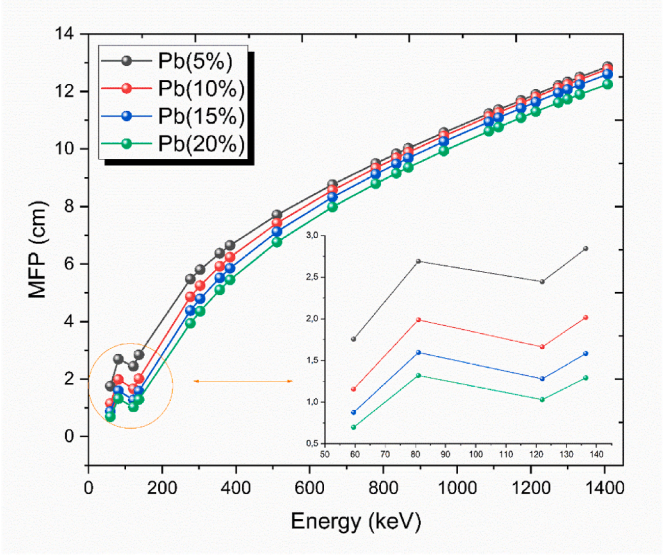

Fig. 10. Mean free path (MFP) values as a function of photon energy.

formed by doping hardener additive to fulfill the reaction and organic peroxide (Cobalt Octoate (6%) as an accelerator into the unsaturated polyester resin. Then, this matrix has been mixed at regular intervals to avoid the phase material collapse in the polymer matrix due to its high unit weight and a homogeneous mixture was tried to obtain. After that, the composites have been fabricated by adding phase material (Pb) with various proportions to the polymer matrix. After curing under suitable conditions (air environment and room temperature) for 28 days, the synthesized polymer composites have been tested to the check their radiation shielding property. The production steps of the Pb polymer composites have been demonstrated in Fig. 1. Table 1 summarizes the chemical compositions and mass densities pertaining to each sample.

3.2. Experimental process

The gamma radiation shielding capabilities of the prepared Pb-doped polyester composite were investigated both experimentally and theoretically using the software programs mentioned in section 3.3. First, the experimental setup shown in Fig. 2 was created. Preamplifier, radioactive source, multi-channel analyzer, high voltage source, linear amplifier, and basic HPGe detector system make up the experimental geometry of the study. Lead collimators were used to alter the beam shape, as indicated in the picture, as well as a sandwich collimator surrounded with Pb, Fe, and Al to decrease potential backgrounds. Aside from that, the trials were carried out with the help of liquid nitrogen to reduce noise and maximize the detection system's performance. After that, radiation intensities were measured using the suggested setup at 22 distinct photon energies range between 59.5 and 1408.0 keV. To experimentally assess ionizing radiation shielding performance of the fabricated polymer-based composites through mass attenuation

Table 4
Equivalent atomic numbers of the Pb doped polymer composites for various energy values ranging from 0.015 to 15 MeV.

Energy (MeV)	Pb (5%)	Pb (10%)	Pb (15%)	Pb (20%)
0.015	11.377	13.524	15.045	16.276
0.02	13.464	16.219	18.157	19.702
0.03	14.283	17.202	19.233	20.823
0.04	14.876	17.897	19.974	21.604
0.05	15.340	18.441	20.558	22.205
0.06	15.720	18.879	21.026	22.695
0.08	16.314	19.571	21.774	23.476
0.1	26.026	31.675	35.505	38.465
0.15	27.628	33.495	37.443	40.479
0.2	28.608	34.594	38.599	41.664
0.3	29.823	35.941	40.012	43.111
0.4	30.558	36.752	40.861	43.975
0.5	31.049	37.287	41.408	44.536
0.6	31.364	37.641	41.780	44.908
0.8	31.712	38.030	42.185	45.317
1	31.828	38.156	42.326	45.467
1.5	25.163	32.937	37.906	41.589
2	14.240	20.796	26.190	30.569
3	10.181	13.790	17.112	20.165
4	9.361	12.245	14.943	17.453
5	9.027	11.625	14.048	16.322
6	8.850	11.283	13.560	15.697
8	8.668	10.931	13.056	15.054
10	8.585	10.771	12.827	14.761
15	8.512	10.635	12.632	14.516

coefficients (μ/ρ), it has been carried out gamma spectrometer equipped with a high purity Germanium (HPGe) detector. The experimental layout of the test setup is shown in Fig. 2. In addition to having a resolution of 0.380 keV at 5.9 keV, 0.585 keV at 122 keV and 1.8 keV at 1330 keV full width at half maximum (FWHM), the HPGe detector has 25 mm active crystal length and a diameter of 70 mm. The HPGe detector was kept at liquid nitrogen that has a temperature of −196 °C during the experiment and the energy calibration for spectrometer was applied through a mixed calibration. ^{241}Am, ^{152}Eu, ^{137}Cs, ^{133}Ba, ^{60}Co, ^{57}Co, ^{54}Mn and ^{22}Na radioactive point sources with photo-peak energies between 59.5 and 1408.0 keV can be utilized (Manohara et al., 2008). The details on gamma spectrometer can be given from previous publications (Özkalaycı et al., 2020; Kacal et al., 2020; Akman et al., 2021; Turhan et al., 2020). The detected photo-peaks in data acquisitions are analyzed using an MAESTRO software (Agar et al., 2017). Also, the areas belonging to photo-peak are checked via the least-squares fitting method through the Origin 7.5 program (demo version).

The following relation is considered for determining the experimental uncertainties in the shielding tests (Akman et al., 1036):

$$\Delta\mu_m = \frac{1}{\rho x}\sqrt{\left(\frac{\Delta I}{I}\right)^2 + \left(\frac{\Delta I_0}{I_0}\right)^2 + \ln\left(\frac{I_0}{I}\right)^2\left(\frac{\Delta\rho x}{\rho x}\right)^2} \quad (13)$$

where ρ specifies the density, ΔI_0 and ΔI represent the uncertainties of original (I_0) and attenuated (I) counts, respectively.

3.3. Theoretical expectations and Monte Carlo simulations

Theoretical calculations derived from photon energy were produced using the WinXCOM software in the second phase of the sample analysis. The relevant parameters for radiation attenuation assessment were accurately calculated and compared to the measurements using the same photon energy range as the experimental study. The theoretical predictions were also used to confirm the actual setup's accuracy. Theoretical expectations and Monte Carlo (MC) simulations are good supportive techniques to experimental results. Even, they sometimes become very useful tools in lack of experimental apparatus. Therefore, their proper usage makes vital contributions to every kind of researches. Recently, there are numerous types of theoretical calculation tool and MC simulations, which serve for different purposes. In this work, theoretical expectations are obtained using WinXCOM (Gerward et al., 2004) code while FLUKA (Böhlen et al., 2014) and GEANT4 (Agostinelli et al., 2003) programs are chosen simulation tools, which are very commonly used techniques in the research and development of radiation shielding materials.

WinXCOM code uses predefined elemental tables (coded by the program developers) and elemental weights of the materials in order to calculate gamma radiation mass attenuation coefficients of the proposed radiation shielding attenuators in unit of cm^2/g. Additionally, the desired radiation energy is required to be encoded into the program. There is no need to provide density or thickness of the considered

Table 5
G-P energy absorption and exposure build-up factor parameters of the Pb (20%) for various energy values ranging from 0.015 to 15 MeV.

Energy (MeV)	EABF					EBF				
	a	b	c	d	Xk	a	b	c	d	Xk
0.015	0.279	1.015	0.323	−0.180	13.976	0.298	1.016	0.322	−0.257	13.190
0.02	0.282	1.019	0.334	−0.199	11.591	0.212	1.018	0.397	−0.102	11.326
0.03	0.239	1.052	0.356	−0.153	13.734	0.220	1.053	0.372	−0.149	14.258
0.04	0.230	1.107	0.366	−0.124	13.866	0.238	1.108	0.356	−0.131	13.359
0.05	0.232	1.186	0.371	−0.134	14.292	0.221	1.175	0.389	−0.124	14.088
0.06	0.209	1.278	0.412	−0.121	14.736	0.200	1.245	0.431	−0.112	14.211
0.08	0.170	1.496	0.493	−0.095	15.398	0.165	1.383	0.510	−0.091	14.429
0.1	0.282	1.238	0.321	−0.149	15.126	0.260	1.189	0.349	−0.140	13.783
0.15	0.279	1.514	0.336	−0.157	14.041	0.167	1.269	0.508	−0.087	14.377
0.2	0.314	2.287	0.315	−0.196	14.017	0.170	1.479	0.521	−0.098	14.275
0.3	0.166	2.316	0.544	−0.100	14.024	0.084	1.561	0.720	−0.044	14.451
0.4	0.118	2.568	0.681	−0.092	13.899	0.045	1.664	0.864	−0.036	14.169
0.5	0.080	2.584	0.788	−0.071	13.890	0.025	1.718	0.942	−0.028	14.239
0.6	0.060	2.554	0.847	−0.060	13.748	0.012	1.738	0.990	−0.021	13.971
0.8	0.037	2.436	0.922	−0.046	13.647	−0.001	1.751	1.041	−0.015	14.051
1	0.025	2.319	0.961	−0.038	13.527	−0.007	1.739	1.063	−0.013	13.430
1.5	−0.011	1.941	1.094	−0.015	13.329	−0.030	1.627	1.162	0.001	7.428
2	−0.016	1.837	1.104	−0.008	9.999	−0.021	1.682	1.122	−0.004	9.429
3	−0.005	1.687	1.050	−0.010	11.966	−0.011	1.640	1.070	−0.007	13.201
4	0.011	1.592	0.988	−0.018	12.699	0.008	1.581	1.002	−0.015	10.768
5	0.018	1.511	0.963	−0.026	14.824	0.013	1.515	0.979	−0.017	12.458
6	0.021	1.446	0.951	−0.029	15.287	0.019	1.469	0.957	−0.021	13.709
8	0.036	1.360	0.912	−0.031	11.815	0.029	1.389	0.928	−0.028	13.657
10	0.038	1.298	0.906	−0.034	13.618	0.038	1.330	0.907	−0.034	13.345
15	0.035	1.197	0.922	−0.035	14.404	0.050	1.235	0.883	−0.047	13.217

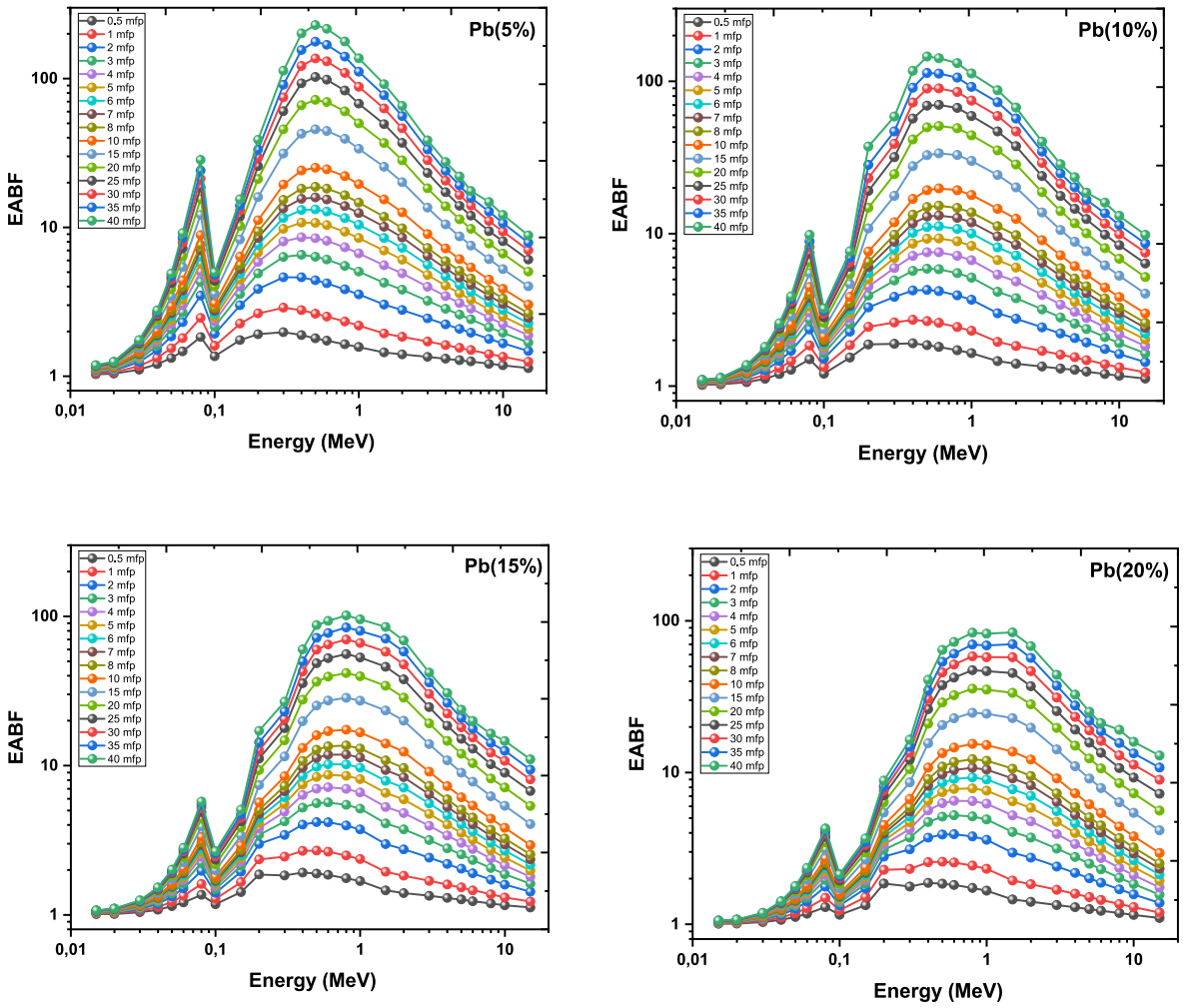

Fig. 11. Energy absorption buildup factors (EABF) against photon energies at various mfp.

material. On the other hand, FLUKA and GEANT4 are the simulation tools to calculate the number of transmitted gamma numbers through the chosen radiation attenuator, which are useful inputs to calculate linear attenuation coefficient as defined mathematically earlier. In both simulation tools, with thickness, density and elemental weight of the materials, the proposed radiation attenuator was modeled and bombarded with 10 000 000 gamma particles. User should also define the considered gamma radiation energy in order to have the gamma attenuation coefficients. In WinXCOM, FLUKA and GEANT4 codes, the gamma energy points were appointed as the same with the experimental choices, which let us to have fruitful comparison between experimental, theoretical and simulation sides.

4. Results and discussions

The linear attenuation coefficients were first calculated and graphed in a three-dimensional graph in order to evaluate the radiation attenuator as indicated in the section on analytical methods (Fig. 3). The attenuation curves reveal that the coefficients fall exponentially when dopant amount enhancement of the produced composite's linear attenuation property and the radiation energy grow. At low energy levels, photoelectric cross section is the dominant process with $E^{-3.5}$ energy dependency and Z^{4-5} atomic number dependency while at mid-levels of energy Compton scattering is the dominant process with E^{-1} energy dependency and Z atomic number dependency. At high energy levels, an exponential decline occurs due to the pair production cross section with energy dependency of E and atomic number dependency of Z^2. Since the linear attenuation is dependent on material density, material attenuation is typically estimated using the μ/ρ ratio. Fig. 4 reports μ/ρ values of the selected samples as a function of energy. To confirm the experimental results, the WinXCOM, FLUKA, and GEANT4 programs were used. The elemental compositions of the composites at various energies ranging from 59.5 to 1408.0 keV were utilized to estimate the theoretical and simulation findings and the obtained results were given in Table 2. As can be seen from Table 2, the results of μ/ρ for the chosen samples are consistent, and they may be used in subsequent calculations to investigate gamma interaction features. This validates the experimental setup's accuracy, indicating that it might be utilized to assess the Pb-doped polyester composites' radiation attenuation. In addition to the setup's precision, the results show that the μ/ρ drops exponentially as the gamma energy increases. In other words, the produced composite's shielding capacity is shown to be higher at low energies. Increasing the Pb dopant quantity increases the mass attenuation coefficient (Fig. 4). This increase is stronger at low energies than the increase at high gamma radiation energies.

At low energies, μ/ρ of the composite with Pb (20%) dopant is twice of the composite with Pb (5%) dopant, but this difference reduces as the energy increases. The coefficients are almost the same for larger levels as well. The TVL and HVL values were also studied since they were both useful indicators of a material's gamma radiation shielding ability. Due to the dependence of the linear attenuation coefficient (μ), both TVL and HVL are a function of gamma radiation energy, as shown in the calculations above. To acquire the appropriate values, the $\ln 2/\mu$ and $\ln 10/\mu$ formulae were fulfilled after the linear attenuation coefficients were

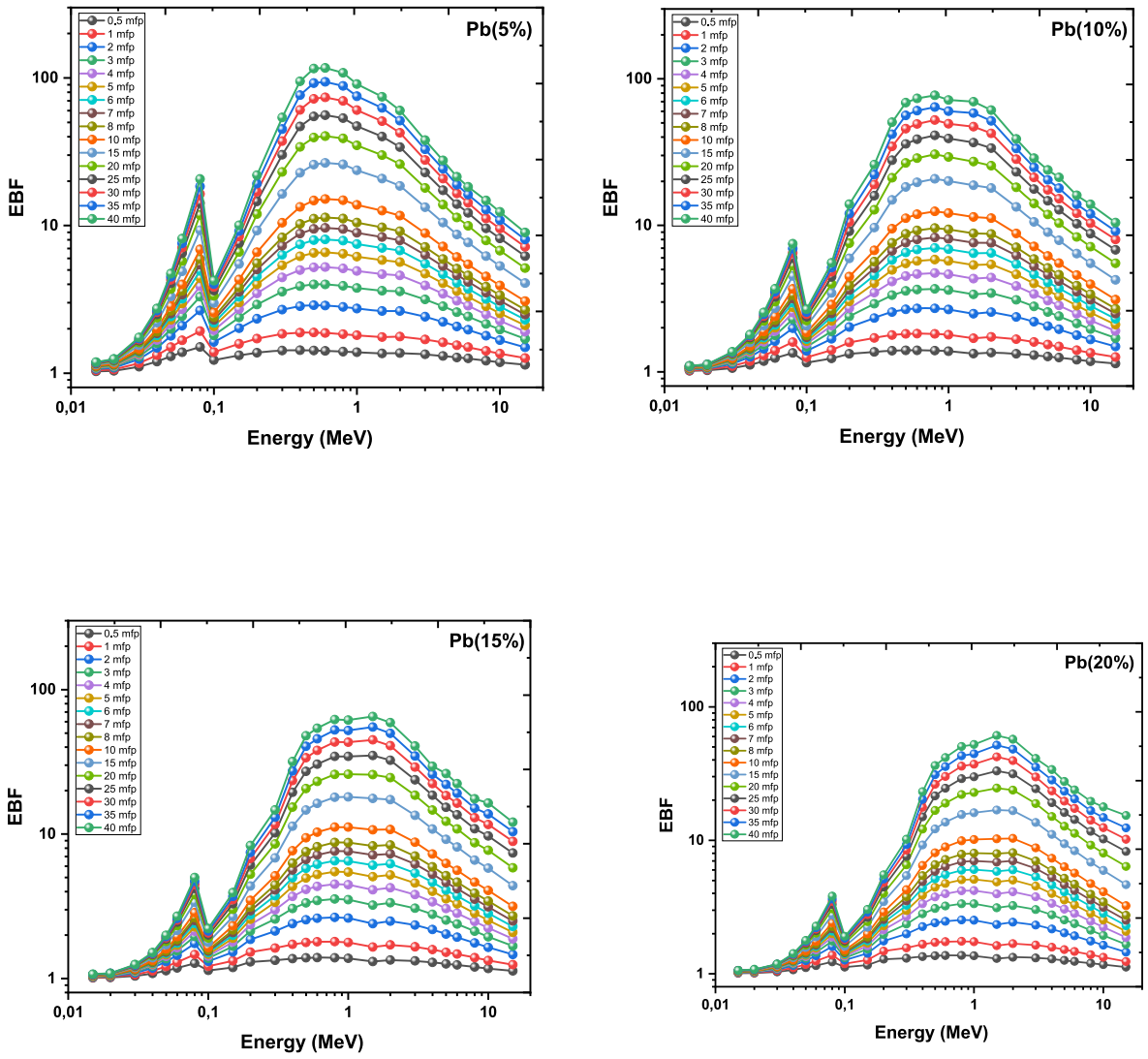

Fig. 12. Exposure buildup factors (EBF) against photon energies at various mfp.

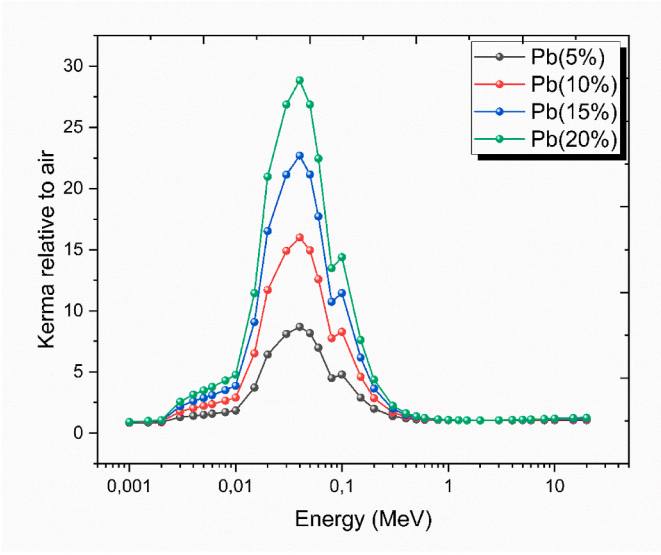

Fig. 13. The change of kerma relative to air against photon energies.

calculated. Figs. 5 and 6 show the results of these computations that show both HVL and TVL increase as radiation energy increases. The HVL value of the samples containing Pb (20%) is lower than the others, indicating that this sample exhibits superior radiation attenuation (Kara et al., 2020a; Kilicoglu, 2019).

The TVL and HVL values of prepared composites were raised in the sequence as Pb (20%) <Pb (15%) < Pb (10%) < Pb (5%). Furthermore, knowing the electron density (N_E) and effective atomic number (Z_{eff}) characteristics are essential for determining the radiation shielding capability of the produced composites. In essence, a high effective atomic number corresponds to a large number of electrons per atom; the two factors are intertwined. Eqs. (6) and (9) are used to compute these parameters and the Z_{eff} and N_E are plotted as shown in Figs. 7 and 8, respectively.

The observed results reveal major disparities among the composites under consideration. As predicted, Z_{eff} and N_E act similarly, and decrease with increasing gamma radiation energy in all samples. Furthermore, there was a significant difference in Z_{eff} values for Pb (5%) and Pb (20%), with the values increasing in the sequence of Pb (5%) <Pb (10%) < Pb (15%) < Pb (20%). In addition, Table 3 gives both the theoretical and experimental Z_{eff} values of the selected samples. That means, the findings of theoretical and experimental Z_{eff} values for the chosen samples are consistent with each other. In this case, all Z_{eff} assessments are also valid for the N_E parameter. According to Z_{eff} and N_E,

Pb (20%) has a superior radiation attenuator property.

The determination of RPE of prepared samples as a function of energy is an essential parameter investigated in this work. It was estimated for four distinct composites with varied amounts of Pb (5%), Pb (10%), Pb (15%) and Pb (20%). Fig. 9 shows the collected data, which clearly illustrate that RPE is inversely proportional to radiation energy. Furthermore, it was discovered that the composite comprised of Pb had the highest RPE value (20%). The MFP parameter is important in terms of exposing the attenuation performance of any material under investigation in order to reduce radiation dosage to an acceptable level for environmental health. Any composite material with a lower MFP value has a more effective shield absorber. The MFP findings for Pb doped polyester composites are shown in Fig. 10. As shown in the figure, the MFP results are linearly dependent on photon energy for the produced composites. The highest and lowest MFP values are Pb (5%) and Pb (20%), respectively, with densities of 1.3903 and 1.4652 g/cm^3 (Table 1). The MFP parameter is simply inferred to be connected to material densities, and hence the ratio of shielding effectiveness to density is proportional.

The five-parameter geometric progression (G-P) fitting approach was used to calculate EBF and EABF for penetration depths up to 40 mfp in the energy ranges from 0.015 MeV to 15 MeV. Table 4 lists the Z_{eq} of Pb doped-polymer-composites with energies ranging from 0.015 to 15 MeV. Table 5 also includes G-P exposure, EBF and EABF values for Pb (20%) between 0.015 and 15 MeV energies. It can be noticed that the EBF and EABF values are initially modest, but they rapidly grow as photon energy increases. Low, medium, and high-level energy areas are commonly used to scale energy levels, each with a different dominant incident and effects. In the low energy area, the photoelectric effect becomes the dominant incident, resulting in an inversely proportional effect with $E^{3.5}$. Because the samples of the selected composites absorb the largest number of low-energy photons, these photons are not allowed to accumulate. Compton scattering becomes dominant incident in the intermediate energy region, resulting in high EBF and EABF values for all selected composites. These high EBF and EABF values aren't due to the MFP, but rather various scattering processes. The pair production process is dominant in the high-energy area, and the EBF and EABF values drop with incident photon energy. Pb (20%) has the highest Z_{eq} value and the lowest EBF and EABF values. Furthermore, as shown in Figs. 11 and 12, the EBF and EABF are inversely related to Z_{eq}, with the lowest Z_{eq} value yielding the largest EBF and EABF value. Furthermore, it should be observed that selected composites (i.e. Pb 5%) with the lowest Z_{eq} yield the highest EABF and EBF, whereas selected composites with the highest Z_{eq} (i.e. Pb 20%) yield the lowest EABF and EBF. That is, Pb (20%) is a more effective gamma-ray shielding composite than Pb (5%). For example, the greatest values of EABF and EBF occur at various level in Pb (5 percent) (the sample's lowest Z_{eq}). Similarly, the lowest values of EABF and EBF occur at varied levels in Pb (20%) (which is the greatest Z_{eq} in the sample).

Fig. 11 shows EABF values for Pb doped-polymer-composites with incoming photon energies of 0.5, 1, 2, 3, 4, 5, 6, 7, 8, 10, 15, 20, 25, 30, 35, and 40 mfp. In addition, EBF values of Pb (5%, 10%, 15%, 20%) doped-polymer-composites were presented in Fig. 12 for penetration depths of 0.5, 1, 2, 3, 4, 5, 6, 7, 8, 10, 15, 20, 25, 30, 35, and 40 mfp between 0.015 and 15 MeV energies (Kara et al., 2020b; Kilicoglu et al., 2021). EABF and EBF values for Pb doped-polymer-composite materials exhibit various characteristic at different energies, as shown in Figs. 11 and 12. The largest values of EABF and EBF are found in the medium energy zone (Compton scattering region). In addition, at 40 mfp, build-up factors reached their highest levels. Fig. 11 shows that EABF-values at 40 mfp indicate a peak at 0.5 MeV for Pb (5%) (229.06), at 0.5 MeV for Pb (10%) (145.58), at 0.8 MeV for Pb (15%) (101.48) and at 1.5 MeV for Pb (20%) (83.89). Fig. 12 shows that EBF-values at 40 mfp indicate a peak at 0.6 MeV for Pb (5%) (116.99), at 0.8 MeV Pb (10%) (77.29), 1.5 MeV for Pb (15%) (65.22) and at 1.5 MeV Pb (20%) (65.11). Pb (5%) has the highest EBF-EABF values in the medium energies in all penetration-depths.

Fig. 13 shows the change of kerma relative to air (K_a) in Pb doped-polymer-composite samples with photon energies ranging from 1 keV to 20 MeV. In the whole energy range of 1 keV–20 MeV, the K_a values of the Pb (5%) are the lowest among all the Pb doped-polymer-composite samples. The variation in K_a values with energy reflect changes in Z_{eff} due to partial photon interaction processes such as photo-absorption, Compton scattering, and pair production. In the photon energy range of 1–20 keV, the K_a values of all the Pb doped-polymer-composite samples are in the range of 0.848–1.255. In the energy range 1–20 keV, however, the K_a values of Pb (5%) were 0.848–1.053.

5. Conclusions

Despite some disadvantages, Pb is still the most effective shielding material and thus, a small amount of Pb has been added to the fabricated polymer composites to shield X- and gamma ray radiation in various applications. In order to confirm the consistency of experimental data, the obtained mass attenuation coefficient values were compared with those estimated by the WinXCOM program as well as FLUKA and GEANT4 simulation codes. There was a good agreement among the experimental measurements, theoretical (WinXCOM) and simulation (FLUKA and GEANT4) calculations. The evaluation of the fabricated composites has studied regarding mass attenuation coefficient, linear attenuation coefficient, HVL, TVL, MFP, Z_{eff}, N_E, RPE, EBF, EABF and K_a. The results show that the prepared polymer-based composites are very good at attenuating photons and the best material among the prepared samples is Pb (20%) polymer-based composite. Thanks to having this new material to attenuate photons, we introduce a new nuclear shielding absorber through minimized lead content in the micro-composite prepared.

Author statement

Özge Kılıçoğlu: Writing-Original Draft, Writing-Review&Editing, Formal analysis.

Chaitali V. More: Writing-Original Draft, Writing-Review&Editing, Formal analysis.

Ferdi Akman: Conceptualization, Formal analysis, Writing-Review&Editing, Supervision, Project administration.

Kamuran Dilsiz: Writing-Original Draft, Writing-Review&Editing, Formal analysis.

Hasan Ogul: Writing-Original Draft, Writing-Review&Editing, Formal analysis.

Mustafa Recep Kaçal: Methodology, Validation, Investigation, Resources.

Hasan Polat: Methodology, Investigation.

Osman Agar: Formal analysis, Data Curation, Writing-Original Draft, Writing-Review&Editing, Formal analysis.

Declaration of competing interest

The authors declare that they have no known competing financial interests or personal relationships that could have appeared to influence the work reported in this paper.

References

Abu-Jdayil, B., Thomas, S., Hosur, M., 2019. In: Chirayil, C.J. (Ed.), Unsaturated Polyester Resins: Fundamentals, Design, Fabrication, and Applications. Elsevier.

Afshar, M., Morshedian, J., Ahmadi, S., 2019. Radiation attenuation capability and flow characteristics of HDPE composite loaded with W, MoS2, and B4C. Polym. Compos. 40 (1), 149–158.

Agar, O., Boztosun, I., Segebade, C., 2017. Multielemental analysis of some soils in Karaman by PAA using a cLINAC. Appl. Radiat. Isot. 122, 57–62.

Agostinelli, S., Allison, J., Amako, K.A., Apostolakis, J., Araujo, H., Arce, P., et al., 2003. GEANT4—a simulation toolkit. Nucl. Instrum. Methods Phys. Res. Sect. A Accel. Spectrom. Detect. Assoc. Equip. 506 (3), 250–303.

Akman, F., Ogul, H., Kaçal, M. R., Polat, H., Dilsiz, K., & Agar, O. Gamma attenuation characteristics of CdTe-Doped polyester composites. Prog. Nucl. Energy, 131, 103608.

Akman, F., Ozkan, I., Kaçal, M.R., Polat, H., Issa, S.A., Tekin, H.O., Agar, O., 2021. Shielding features, to non-ionizing and ionizing photons, of FeCr-based composites. Appl. Radiat. Isot. 167, 109470.

Alavian, H., Tavakoli-Anbaran, H., 2020. Comparative study of mass attenuation coefficients for LDPE/metal oxide composites by Monte Carlo simulations. Eur. Phys. J. Plus 135 (1), 82.

Aldhuhaibat, M.J., Amana, M.S., Jubier, N.J., Salim, A.A., 2021. Improved gamma radiation shielding traits of epoxy composites: evaluation of mass attenuation coefficient, effective atomic and electron number. Radiat. Phys. Chem. 179, 109183.

Ambika, M.R., Nagaiah, N., Suman, S.K., 2017. Role of bismuth oxide as a reinforcer on gamma shielding ability of unsaturated polyester based polymer composites. J. Appl. Polym. Sci. 134 (13).

Azman, N.N., Siddiqui, S.A., Hart, R., Low, I.M., 2013. Effect of particle size, filler loadings and x-ray tube voltage on the transmitted x-ray transmission in tungsten oxide—epoxy composites. Appl. Radiat. Isot. 71 (1), 62–67.

Bagheri, K., Razavi, S.M., Ahmadi, S.J., Kosari, M., Abolghasemi, H., 2018. Thermal resistance, tensile properties, and gamma radiation shielding performance of unsaturated polyester/nanoclay/PbO composites. Radiat. Phys. Chem. 146, 5–10.

Bedar, A., Lenka, R.K., Goswami, N., Kumar, V., Debnath, A.K., Sen, D., Kumar, S., Ghodke, S., Tewari, P.K., Bindal, R.C., Kar, S., 2019. Polysulfone–ceria mixed-matrix membrane with enhanced radiation resistance behavior. ACS Appl. Polym. Mater. 1 (7), 1854–1865.

Belgin, E.E., Aycik, G.A., Kalemtas, A., Pelit, A., Dilek, D.A., Kavak, M.T., 2015. Preparation and characterization of a novel ionizing electromagnetic radiation shielding material: hematite filled polyester based composites. Radiat. Phys. Chem. 115, 43–48.

Böhlen, T.T., Cerutti, F., Chin, M.P.W., Fassò, A., Ferrari, A., Ortega, P.G., Mairani, A., Sala, P.R., Smirnov, G., Vlachoudis, V., 2014. The FLUKA code: developments and challenges for high energy and medical applications. Nucl. Data Sheets 120, 211–214.

Gerward, L., Guilbert, N., Jensen, K.B., Levring, H., 2004. WinXCom—a program for calculating X-ray attenuation coefficients. Radiat. Phys. Chem. 71 (3–4), 653–654.

Harish, V., Nagaiah, N., Prabhu, T.N., Varughese, K.T., 2009. Preparation and characterization of lead monoxide filled unsaturated polyester based polymer composites for gamma radiation shielding applications. J. Appl. Polym. Sci. 112 (3), 1503–1508.

Harish, V., Nagaiah, N., Prabhu, T.N., Varughese, K.T., 2010. Thermo-mechanical analysis of lead monoxide filled unsaturated polyester based polymer composite radiation shields. J. Appl. Polym. Sci. 117 (6), 3623–3629.

Harish, V., Nagaiah, N., Kumar, H.G., 2012. Lead Oxides Filled Isophthalic Resin Polymer Composites for Gamma Radiation Shielding Applications.

Hassan, H.E., Badran, H.M., Aydarous, A., Sharshar, T., 2015. Studying the effect of nano lead compounds additives on the concrete shielding properties for γ-rays. Nucl. Instrum. Methods Phys. Res. Sect. B Beam Interact. Mater. Atoms 360, 81–89.

Hubbell, J., Seltzer, S., 1995. Tables of X-ray mass attenuation coefficients and mass energy-absorption coefficients 1 keV to 20 MeV for elements Z = 1 to 92 and 48 additional substances of dosimetric interest [online]. http://physics.nist.gov/PhysRefData/XrayMassCoef/cover.html. http://physics.nist.gov/PhysRefData/XrayMassCoef/cover.html (Accessed June 20, 2021).

Kacal, M.R., Polat, H., Oltulu, M., Akman, F., Agar, O., Tekin, H.O., 2020. Gamma shielding and compressive strength analyses of polyester composites reinforced with zinc: an experiment, theoretical, and simulation based study. Appl. Phys. A 126 (3), 1–15.

Kara, U., Kilicoglu, O., Karaibrahimoglu, A., Cavdarli, K., Ince, F., 2020a. Radiation attenuation properties of removable partial dentures (RPD). Mater. Chem. Phys. 253, 123301.

Kara, U., Kilicoglu, O., Ersoy, S., 2020b. Structural and gamma-ray attenuation coefficients of different OAD films for nuclear medicine applications. Radiat. Phys. Chem. 172, 108785.

Kaçal, M.R., Akman, F., Sayyed, M.I., Akman, F., 2019. Evaluation of gamma-ray and neutron attenuation properties of some polymers. Nucl. Eng. Technol. 51 (3), 818–824.

Kilicoglu, O., 2019. Characterization of copper oxide and cobalt oxide substituted bioactive glasses for gamma and neutron shielding applications. Ceram. Int. 45 (17), 23619–23631.

Kilicoglu, O., Kara, U., Inanc, I., 2021. The impact of polymer additive for N95 masks on gamma-ray attenuation properties. Mater. Chem. Phys. 260, 124093.

Kumar, A., Gaikwad, D.K., Obaid, S.S., Tekin, H.O., Agar, O., Sayyed, M.I., 2020. Experimental studies and Monte Carlo simulations on gamma ray shielding competence of (30+ x) PbO10WO3 10Na2O− 10MgO–(40-x) B2O3 glasses. Prog. Nucl. Energy 119, 103047.

Manohara, S.R., Hanagodimath, S.M., Gerward, L., 2008. Studies on effective atomic number, electron density and kerma for some fatty acids and carbohydrates. Phys. Med. Biol. 53 (20), N377.

Mansy, M.S., Lasheen, Y.F., Breky, M.M., Selim, Y., 2021. Experimental and theoretical investigation of Pb–Sb alloys as a gamma-radiation shielding material. Radiat. Phys. Chem. 183, 109416.

More, C.V., Pawar, P.P., Badawi, M.S., Thabet, A.A., 2020a. Extensive theoretical study of gamma-ray shielding parameters using epoxy resin-metal chloride mixtures. Nucl. Technol. Radiat. Protect. 35 (2), 138–149.

More, C.V., Alavian, H., Pawar, P.P., 2020b. Evaluation of gamma-ray attenuation characteristics of some thermoplastic polymers: experimental, WinXCom and MCNPX studies. J. Non-Cryst. Solids 546, 120277.

More, C.V., Alsayed, Z., Badawi, M.S., Thabet, A.A., Pawar, P.P., 2021. Polymeric composite materials for radiation shielding: a review. Environ. Chem. Lett. 1–34.

Özdemir, T., Güngör, A., Akbay, I.K., Uzun, H., Babucçuoglu, Y., 2018. Nano lead oxide and epdm composite for development of polymer based radiation shielding material: gamma irradiation and attenuation tests. Radiat. Phys. Chem. 144, 248–255.

Özkalaycı, F., Kaçal, M.R., Agar, O., Polat, H., Sharma, A., Akman, F., 2020. Lead (II) chloride effects on nuclear shielding capabilities of polymer composites. J. Phys. Chem. Solid. 145, 109543.

Sharma, A., Sayyed, M.I., Agar, O., Kaçal, M.R., Polat, H., Akman, F., 2020. Photon-shielding performance of bismuth oxychloride-filled polyester concretes. Mater. Chem. Phys. 241, 122330.

Singh, N., Singh, K.J., Singh, K., Singh, H., 2004. Comparative study of lead borate and bismuth lead borate glass systems as gamma-radiation shielding materials. Nucl. Instrum. Methods Phys. Res. Sect. B Beam Interact. Mater. Atoms 225 (3), 305–309.

Singh, V.P., Badiger, N.M., Kaewkhao, J., 2014. Radiation shielding competence of silicate and borate heavy metal oxide glasses: comparative study. J. Non-Cryst. Solids 404, 167–173.

Tekin, H.O., Kavaz, E., Papachristodoulou, A., Kamislioglu, M., Agar, O., Guclu, E.A., et al., 2019. Characterization of SiO2–PbO–CdO–Ga2O3 glasses for comprehensive nuclear shielding performance: alpha, proton, gamma, neutron radiation. Ceram. Int. 45 (15), 19206–19222.

Turhan, M.F., Akman, F., Polat, H., Kaçal, M.R., Demirkol, İ., 2020. Gamma-ray attenuation behaviors of hematite doped polymer composites. Prog. Nucl. Energy 129, 103504.

Vahabi, S.M., Zafarghandi, M.S., 2020. Build-up factors for water and soft tissue by MCNP using a co-centric multilayer model: comparative study. J. Instrum. 15 (5), P05018.